AD-A140 164 ESTIMATING SPECTRAL INDICES FROM TRANSFORMS OF DISCRETE 1/1
REPRESENTATIONS OF DENSITY FUNCTIONS(U) NAVAL RESEARCH
LAB WASHINGTON DC M MULBRANDON ET AL. 30 MAR 84
UNCLASSIFIED NRL-MR-5298 F/G 17/8 NL

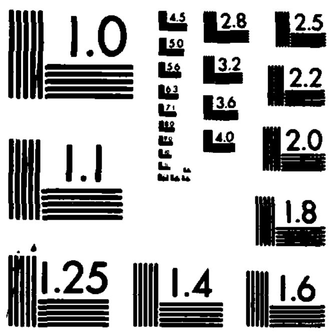

MICROCOPY RESOLUTION TEST CHART
NATIONAL BUREAU-OF STANDARDS-1963-A

(2)

NRL Memorandum Report 5298

Estimating Spectral Indices from Transforms of Discrete Representations of Density Functions

M. MULBRANDON, N.J. ZABUSKY* AND E. HYMAN**

Geophysical and Plasma Dynamics Branch
Plasma Physics Division

**Fluid Sciences, Inc.*
Pittsburgh, PA 15217

***Science Applications, Inc.*
McLean, VA 22102

March 30, 1984

This research was supported by the Defense Nuclear Agency under Subtask S99QMXBI, work unit 00018 and work unit title "IR Structure."

NAVAL RESEARCH LABORATORY
Washington, D.C.

SECURITY CLASSIFICATION OF THIS PAGE

REPORT DOCUMENTATION PAGE

- **1a. REPORT SECURITY CLASSIFICATION:** UNCLASSIFIED
- **1b. RESTRICTIVE MARKINGS:**
- **2a. SECURITY CLASSIFICATION AUTHORITY:**
- **2b. DECLASSIFICATION/DOWNGRADING SCHEDULE:**
- **3. DISTRIBUTION/AVAILABILITY OF REPORT:** Approved for public release; distribution unlimited.
- **4. PERFORMING ORGANIZATION REPORT NUMBER(S):** NRL Memorandum Report 5298
- **5. MONITORING ORGANIZATION REPORT NUMBER(S):**
- **6a. NAME OF PERFORMING ORGANIZATION:** Naval Research Laboratory
- **6b. OFFICE SYMBOL (If applicable):**
- **7a. NAME OF MONITORING ORGANIZATION:**
- **6c. ADDRESS (City, State and ZIP Code):** Washington, DC 20375
- **7b. ADDRESS (City, State and ZIP Code):**
- **8a. NAME OF FUNDING/SPONSORING ORGANIZATION:** Defense Nuclear Agency
- **8b. OFFICE SYMBOL (If applicable):**
- **9. PROCUREMENT INSTRUMENT IDENTIFICATION NUMBER:**
- **8c. ADDRESS (City, State and ZIP Code):** Washington, DC 20305
- **10. SOURCE OF FUNDING NOS.**

PROGRAM ELEMENT NO.	PROJECT NO.	TASK NO.	WORK UNIT NO.
62715H			47-0917-04

- **11. TITLE (Include Security Classification):** (See Page ii)
- **12. PERSONAL AUTHOR(S):** M. Mulbrandon, N.J. Zabusky* and E. Hyman**
- **13a. TYPE OF REPORT:** Interim
- **13b. TIME COVERED:** FROM TO
- **14. DATE OF REPORT (Yr., Mo., Day):** March 30, 1984
- **15. PAGE COUNT:** 41
- **16. SUPPLEMENTARY NOTATION:** *Fluid Sciences, Inc., Pittsburgh, PA 15217
  **Science Applications, Inc., McLean, VA 22102 (Continues)
- **17. COSATI CODES**

FIELD	GROUP	SUB. GR.

- **18. SUBJECT TERMS (Continue on reverse if necessary and identify by block number):** Power Spectral Density (PSD); Spatial irregularities; Optical scans; Plasma striations (Continues)
- **19. ABSTRACT (Continue on reverse if necessary and identify by block number)**

Structuring of plasma in the high altitude disturbed atmosphere can adversely impact the operation of optical detectors. ~~In~~ this paper ~~we~~ consider idealized functions of one variable that may represent "scan" functions that are obtained from three-dimensional optical sources observed by remote sensors. We establish the relationship between singular properties of these functions or their derivatives and the spectral index of their transforms, and describe the limitations on obtaining reliable spectral indices where there is no clear *separation of scales* in a spatial profile. The ability to extract a good estimate of the spectral index depends on the complexity of the spatial emission profile, the adequacy of resolution, and aliasing errors that necessarily result from the analysis. We illustrate these competitive effects by numerical examples using spatial profiles of a top hat, circular arc and trapezoid.

- **20. DISTRIBUTION/AVAILABILITY OF ABSTRACT:** UNCLASSIFIED/UNLIMITED X SAME AS RPT. ☐ DTIC USERS ☐
- **21. ABSTRACT SECURITY CLASSIFICATION:** UNCLASSIFIED
- **22a. NAME OF RESPONSIBLE INDIVIDUAL:** M. Mulbrandon
- **22b. TELEPHONE NUMBER (Include Area Code):** (202) 767-6781
- **22c. OFFICE SYMBOL:** Code 4780

DD FORM 1473, 83 APR EDITION OF 1 JAN 73 IS OBSOLETE.

SECURITY CLASSIFICATION OF THIS PAGE

11. TITLE (Include Security Classification)

ESTIMATING SPECTRAL INDICES FROM TRANSFORMS OF DISCRETE REPRESENTATIONS OF DENSITY FUNCTIONS

16. SUPPLEMENTARY NOTATION (Continued)

This research was supported by the Defense Nuclear Agency under Subtask S99QMXBI, work unit 00018 and work unit title "IR Structure."

18. SUBJECT TERMS (Continued)

Spectral indices
Separation of scales

CONTENTS

ESTIMATING SPECTRAL INDICES FROM TRANSFORMS OF DISCRETE REPRESENTATIONS OF DENSITY FUNCTIONS

1. INTRODUCTION

One of the important needs of the defense community is to be able to evaluate reliably the effect on optical sensors of the disturbed atmosphere resulting from a high altitude nuclear event (HANE). If we can understand the structure and emission characteristics of the disturbed atmosphere it will be possible to design detectors which avoid particular wavelength regions and can discriminate between targets and artifactual atmospheric phenomena.

A great deal has been learned in the past several years from the research programs at the Naval Research Laboratory (NRL) and elsewhere about the instability mechanisms that lead to ionospheric plasma structures and the space-time characteristics of the resulting striations. In the near future we hope to clarify the cause of the so-called "freezing" phenomenon for striations, make predictions about their inner scale length, etc. However, to use this information to design better detectors, we must relate the observed spectral characteristics of the density fluctuations of the emitting medium to the structures that numerical simulations and other forms of data (besides optical) predict, and vice-versa. This is an "inverse" problem and can be ill-posed and yield nonunique solutions. The motivation for our studies is to reduce nonuniqueness, etc. through a detailed consideration of the procedures used in relating observed spectral quantities to striation properties.

We will address several aspects of this problem in a series of papers that are currently in preparation. In this paper we consider idealized "scan" functions, namely functions of one variable that can arise from

Manuscript approved January 24, 1984.

three-dimensional optical sources that are observed by remote sensors. We will establish the relationship between continuity properties of these functions or their derivatives and the spectral index of their transforms. We will show how inadequate resolution, whether in measured data or numerical simulations, introduces errors in estimates of spectral indices. Specifically, we will discuss the errors that arise from "aliasing" and the number of data samples required to obtain an adequate separation of scales. We will illustrate these effects with numerical examples.

In a second paper in preparation we relate spectral properties of multidimensional emitting sources to spectral properties of the scan functions. Sources of constant emission intensity and sources with finite gradients viewed from different directions will be considered.

In a third paper, a simple model of a realistic nonaxisymmetric ionospheric striation is constructed, which incorporates the properties of emitting structures established in the NRL research programs. Using this model, we examine the variation in spectral properties that would be observed by scans obtained from different viewing directions. We also investigate the sensitivity of the spectral index to variations in model parameters. Subsequent papers will investigate multiple striation effects and other properties needed to further clarify the relationship between emitting sources and measured spectral indices.

A preliminary investigation of these topics has been given by Wortman and Kilb [1]. They have added the additional feature of a self-similar and probabilistic distribution of scale sizes in the density function and a thorough cómparison with available data. However, they do not focus on uncertainties in the spectral indices resulting from inadequate resolution and the inadequate separation of scales.

2. NOTATION AND TRANSFORMS

2.1 Notation

We define the direct and inverse Fourier transforms

$$\hat{f} = \mathcal{F} f \quad \text{and} \quad f = \mathcal{F}^{-1} \hat{f}.$$

Three forms of f are considered. The continuous function on $x \in [-\infty, \infty]$; the periodic function on $x \in [-L, L]$; and the sampled periodic function on $x \in [-L, L]$, with 2N samples and spacing h. These and the relevant forms of Parseval's relation are:

$$\hat{f}(k) = \int_{-\infty}^{+\infty} f(x)\, e^{-ikx} dx, \qquad x \in [-\infty, +\infty], \tag{2.1a}$$

$$f(x) = (2\pi)^{-1} \int_{-\infty}^{+\infty} \hat{f}(k)\, e^{+ikx} dx, \tag{2.1b}$$

$$\int_{-\infty}^{+\infty} |\hat{f}|^2\, dk = 2\pi \int_{-\infty}^{+\infty} f^2(x)\, dx; \tag{2.1c}$$

$$\hat{f}_\nu \equiv \hat{f}(k_\nu) = (2L)^{-1} \int_{-L}^{L} f(x)\, e^{-ik_\nu x}\, dx, \qquad x \in [-L, L]; \tag{2.2a}$$

$$f(x) = \sum_{-\infty}^{+\infty} \hat{f}(k_\nu)\, e^{+ik_\nu x}, \qquad \nu \in [-\infty, +\infty] \tag{2.2b}$$

$$\sum_{-\infty}^{+\infty} |\hat{f}_\nu|^2 = (2L)^{-1} \int_{-\infty}^{+\infty} f^2(x)\, dx \tag{2.2c}$$

$$\hat{F} \equiv \hat{F}(k_\nu) = (2N)^{-1} \sum_{n=-N+1}^{n=N} f(nh)\, e^{-inhk_\nu}, \quad n \in [-N+1, N]; \tag{2.3a}$$

$$f(nh) = \sum_{\nu=-N+1}^{N} \hat{F}(k_\nu)\, e^{+inhk_\nu}, \qquad \nu \,\varepsilon\, [-N+1, N], \tag{2.3b}$$

$$\sum_{\nu=-N+1}^{N} |\hat{F}|^2 = (2N)^{-1} \sum_{n=-N+1}^{N} |f(nh)|^2, \tag{2.3c}$$

where $k_\nu = (\pi\nu/L) \equiv (\pi\nu/Nh)$, and ν is the mode number. Note if $f(x)$ in (2.2a) is a function that vanishes identically outside a region contained within $(-L, L)$, (a function of compact support), then

$$\hat{f}(k)|_{k=k_\nu} = (2L)\, \hat{f}_\nu .$$

That is, they have the same form.

We have displayed these forms so as to clarify relationships. Brigham [2] shows analytically and with lucid graphics that a periodic function $f(x) = f(x+2L)$ can be obtained from a function of compact support on $x \,\varepsilon\, [-L, L]$ by convolving it with the series

$$\sum_{n=-\infty}^{+\infty} \delta(x-2nL).$$

In the transform domain this convolution becomes a product of $\hat{f}(k)$ with $\sum \delta(k-n/2L)$ which amounts to selecting discrete lines from the continuous Fourier transform. Finally, we sample the physical space by multiplying by $\sum \delta(x-nh)$ and integrating. In the transform domain this becomes a convolution which causes the leakage or "aliasing" phenomenon that arises in discrete systems.

2.2 Transforms of Elementary Continuous Functions of Compact Support

One of our goals is to characterize physical space functions by spectral indices. That is, the power density $|\hat{f}|^2$ (or $|\hat{F}|^2$, etc.) has an envelope that may be characterized by k^{-p_j} in various regions j and we seek to define these regions and find accurate estimates of p_j. For convenience in illustrating separation of scales and asymptotic properties, we will use a function f(x) that is composed of piecewise-constant, linear, quadratic, etc. functions and fractional powers of these functions. We believe these functions are sufficiently general to include the essential features of real scans. The spectral index p will be determined by the particular functions that are chosen and by the manner in which they intersect.

First, consider the transform of $(\partial_x f)$ on $x \varepsilon [-\infty, \infty]$

$$\mathcal{F}(\partial_x f) = \int_{-\infty}^{+\infty} (\partial_x f)\, e^{-ikx} dx = (ik)\, \hat{f}(k). \tag{2.4}$$

In general, if $\partial_x^q f$ vanishes sufficiently rapidly, then

$$(\partial_x^q f) = (ik)^q\, \hat{f}(k). \tag{2.5}$$

In the sense of generalized functions, the derivative of a Heaviside step function

$$H(x) = \begin{cases} 1 & x > 0 \\ 1 & x < 0 \end{cases},$$

is the delta function $\delta(x)$. Their transforms are related by $\mathcal{F}(\delta(x)) = 1 = (ik)\, \hat{H}$. Thus, for functions of compact support that are composed of

piecewise polynomials, one differentiates a sufficient number of times until delta and more singular generalized functions are obtained. (For example, for a trapezoid one differentiates twice). To obtain the transform of f, we divide the transforms of these singular functions with singularities located at x_{sj} by the appropriate power of (ik) (the number of differentiations) and combine with appropriate phase shift factors, exp-(ikx_{sj}). Some typical results are given in Table I.

Table 1 — Fourier transforms of elementary figures

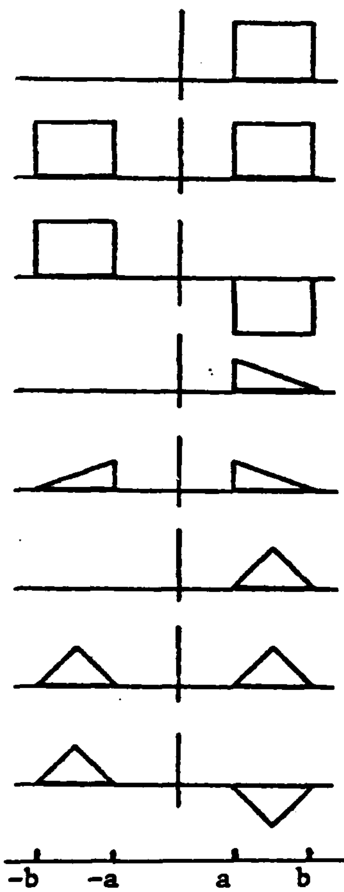

P	Transform	
(2)	$2Ak^{-1} e^{-iz_+} \sin z_-$	(I.1)
(2)	$4Ak^{-1} \cos z_+ \sin z_-$	(I.2)
(2)	$4Ak^{-1} \sin z_+ \sin z_-$	(I.3)
(2)	$iA[-k^{-1} e^{-ika} + 2\Delta^{-1} k^{-2} e^{-iz_+} \sin z_-]$	(I.4)
(2)	$-2Ak^{-1} \sin ka + 4A\Delta^{-1} k^{-2} \sin z_+ \sin z_-$	(I.5)
(4)	$8A\Delta^{-1} k^{-2} e^{-iz_+} \sin^2(z_-/2)$	(I.6)
(4)	$16A\Delta^{-1} k^{-2} \cos z_+ \sin^2(z_-/2)$	(I.7)
(4)	$i16A\Delta^{-1} k^{-2} \sin z_+ \sin^2(z_-/2)$	(I.8)

$$z_\pm = \frac{1}{2}(b \pm a), \quad \Delta = (b - a)$$

The symmetrical trapezoid of amplitude A is obtained by combining (I.5) with (I.2) where in the latter, a = 0 and b = a. Thus

$$\hat{f} = A(b + a)(\sin z_+ \sin z_-)/(z_+ z_-), \tag{2.6}$$

where

$$z_{\pm} = \frac{1}{2} k(b \pm a). \tag{2.7}$$

The half-width of the trapezoid may be defined as $\ell_{1/2} = (b + a)/2$, and the first null of (2.6) is at $\pi/\ell_{1/2}$. This is also the interval between nulls associated with $\sin z_+$. In a similar fashion, if f is

$$
\begin{aligned}
f(x) &= 1, && |x| < a, \\
f(x) &= \left[1 - \left(|x| - a\right)^2/\Delta^2\right]^{\tau}, && a < |x| < b, \qquad (2.8)\\
f(x) &= 0, && |x| > b,
\end{aligned}
$$

where $\Delta = (b - a)$, $\tau > -1$. Note, f is singular at $|x| = b$ if $-1 < \tau < 0$ and f has a singular slope at $|x| = b$ if $0 < \tau < 1$. The transform is given in Appendix A and for $\tau = 1/2$ (an elliptical arc) it is

$$\hat{f}(k) = k^{-1} \sin ka\{2 - \pi\, \underset{\sim}{H}_1(k\Delta)\} + \pi\, k^{-1}\, J_1(k\Delta), \tag{2.9}$$

where $\underset{\sim}{H}_1$ is a Struve function, as discussed, for example, in Reference 3, and J_1 is the Bessel function of the first kind. If $k\Delta >> 1$,

$$\underset{\sim}{H}_1(k\Delta) = Y_1(k\Delta) + \frac{2}{\pi} + O(k\Delta)^{-2},$$

where Y_1 is the Bessel function of the second kind. Thus

$$\lim_{k\Delta >> 1} \hat{f}(k) = (2\pi)^{1/2}\Delta(k\Delta)^{-3/2}\left[\cos\left(k\Delta - \frac{3\pi}{4}\right) - \sin\left(k\Delta - \frac{3\pi}{4}\right)\sin ka\right]. \tag{2.10}$$

Further properties of these functions are discussed below.

3. ASYMPTOTIC SPECTRA AND SEPARATION OF SCALES

3.1 Functions on the Infinite Line

In this section, quantitative results for special functions are presented and general rules are induced. Particularly, that the asymptotic spectrum of continuous functions is determined by the physical space regions where slopes of f change in the most singular manner.

The spectral representation of variables, $|\hat{f}|^2$, in nonlinear dynamical processes often can be represented by a power-law function k^{-p_j} in the region $k_{j-1} < k < k_j$, where p_j is called the spectral index in region j. (This excludes the dissipative range where some exponential variation with k usually occurs). These representations are often obtained by least-squares fitting procedures which suppress oscillatory effects. For example, the <u>envelope</u> of <u>maxima</u> of piecewise polynomials discussed previously can be fitted by $|\hat{f}_e|^2 \propto k^{-p}$ when length scales are sufficiently "separated". For $k \to \infty$, p is called the asymptotic spectral index.

For the trapezoid (2.6), the asymptotic spectrum is $(4/\Delta)^2 k^{-4}$, or p = 4 and for (2.8), the asymptotic spectral index is obtained from Appendix A as

$$p = 2(\tau + 1), \quad \tau > -1. \tag{3.1}$$

For $\tau = 1/2$ (see Equation (2.10)) $p = 3$ which is intermediate between 2 and 4, the values for the top hat and the trapezoid, respectively. For $-1 < \tau < 0$, f is singular at $x = b$ and $0 < p < 2$ (that is, shallower than a top hat). For $0 < \tau < 1$, $f'(x)$ is singular at $x = b$ and for $\tau \geq 1$, $f'(x)$ is everywhere continuous and vanishes at $x = b$. From these results, we induce a rule for piecewise polynomials and powers of piecewise polynomials: the asymptotic spectral index is determined by the nature of the singularities of $\partial^q f/\partial x^q$, where these piecewise polynomials intersect. For example, if the first derivative ($q = 1$) has a singular slope somewhere, then

$$2 \leq p < 4;$$

if $q = 1$ does not have a singular slope but $q = 2$ does have a singularity, then

$$4 \leq p < 6; \text{ etc.}$$

Let us now consider the separation of scales, namely different spectral indices p_j in different regions of k, $k_{j-1} < k \leq k_j$. For the trapezoid (2.6) we have three regions:

$$\begin{aligned} \hat{f}_e(k) &\approx (b + a), & k &\ll k_1, \\ \hat{f}_e(k) &\approx 2k^{-1}, & k_1 \ll k &\ll k_2, \qquad (3.2) \\ \hat{f}_e(k) &\approx (b - a)^{-1}\, k^{-2}, & k_2 &\ll k, \end{aligned}$$

where $k_1 = 2\pi/(b + a)$ and $k_2 = 2\pi/(b - a)$. Thus if $(b + a)/(b - a) \gg 1$ we have a good separation of scales. For the trapezoid-plus-top hat with $\mu \ll 1$ shown in Figure 1,

$$\hat{f} = (1 - \mu)(b + a)(\sin z_+ \sin z_-)/(z_+ z_-) + 2\mu b(\sin kb)/(kb), \qquad (3.3)$$

and we have four regions

$$\begin{aligned}
\hat{f}_e &\approx (1 - \mu)(b + a), & k &\ll k_1, \\
\hat{f}_e &\approx 2k^{-1}, & k_1 &\ll k \ll k_2, \\
\hat{f}_e &\approx (b - a)^{-1}\, k^{-2}, & k_2 &\ll k \ll k_3, \\
\hat{f}_e &\approx 2\mu k^{-1}, & k_3 &\ll k;
\end{aligned} \qquad (3.4)$$

where

$$\begin{aligned}
&k_1 = 2\pi/(b + a),\ k_2 = 2\pi/(b - a), \\
&k_3 = (1 - \mu)\, \mu^{-1}\, \pi/(b - a),
\end{aligned} \qquad (3.5)$$

and where we have assumed $\mu \ll 1$. The asymptotic spectral index is 2 because of the small but finite jump. Note that the last region begins at a point dependent on the size of the discontinuity, which in practice could be related to a data artifact.

3.2 Periodic Continuous and Discrete Functions

Because of the computational efficiency of the fast Fourier transform algorithm, one usually imbeds functions in a periodic domain, $-L < x < L$. If the functions have compact support over a range $< 2L$, then from (2.2a) the transforms have the same form but the continuous k is replaced by $k_\nu = \pi\nu/L$, where ν takes on all positive and negative integers. As a rule, if one wishes many harmonics between nulls, one requires $(L/\ell_{1/2}) \gg 1$, where $\ell_{1/2}$ is the "half-width" of the function. If we satisfy this criterion we will obtain a reasonable approximation to the continuous transform function but it may not yield a good estimate for the spectral index, as we will see in Section 3.3.

For discrete functions, defined at intervals $h = L/N$, Eq. (2.3a) is applicable. The discrete system has 2N independent harmonics $\nu = (-N+1), (-N+2)\ldots-1,0,1,\ldots N$. The lowest harmonic is (π/Nh) and the highest is (π/h). For the symmetric trapezoid, Eq. (2.3a) yields

$$\hat{F}(\theta) = A\,\frac{(\beta+\alpha)}{2N}\left\{\frac{\sin\frac{1}{2}\,\theta(\beta+\alpha)}{(\beta+\alpha)\sin\left(\frac{1}{2}\,\theta\right)}\;\frac{\sin\frac{1}{2}\,\theta(\beta-\alpha)}{(\beta-\alpha)\sin\left(\frac{1}{2}\,\theta\right)}\right\} \tag{3.6}$$

where

$$b = \beta h \text{ and } a = \alpha h, \tag{3.7a}$$

$$\theta = kh = \pi\nu/N, \quad \nu\,\epsilon[-N+1,N], \tag{3.7b}$$

and $\theta_{max} = \pi$. The essential difference between (3.7) and (2.6) is the presence in the denominator of $(\sin\theta/2)^2$ instead of $(\theta/2)^2$. This difference is called "aliasing" [4] and is the result of "folding" the discrete spectrum of the Fourier series around the highest mode. Thus

aliasing, an unavoidable result of dealing with discrete data, modifies the asymptotic spectral index.

To obtain a quantitative measure of the error we define a ratio of local "indices" and subtract one, or

$$\varepsilon_p(\theta) \equiv \left\{\frac{d[\ln|\hat{f}_e|^2]/d(\ln \theta)}{d[\ln|\hat{F}_e|^2]/d(\ln \theta)} - 1\right\}. \tag{3.8}$$

where $\hat{f}_e$ and $\hat{F}_e$ are the envelope functions corresponding to $\hat{f}$ and $\hat{F}$, respectively. Thus if $\varepsilon_p(\theta) > 0$, $\hat{F}_e$ has a smaller effective p than does $\hat{f}_e$. An approximate result for the trapezoid is obtained by setting

$$|\hat{f}_e|^2 = \left(\tfrac{1}{2}\,\theta\right)^{-p_j} \text{ and } |\hat{F}_e|^2 = \left(\sin \tfrac{1}{2}\,\theta\right)^{-p_j},$$

where

$$p_2 = 2 \text{ for } 2\pi/(b+a) \ll k \ll 2\pi/(b-a)$$

$$p_3 = 4 \text{ for } k \gg 2\pi/(b-a).$$

Thus

$$\varepsilon_p = \left[\left(\tan \tfrac{1}{2}\,\theta\right)/\left(\tfrac{1}{2}\,\theta\right)\right] - 1 = \left(\theta^2/12\right) + O\left(\theta^4\right). \tag{3.9}$$

is positive and independent of p_j and is: 0.024 at $\theta = \pi/6$; 0.055 at $\theta = \pi/4$; 0.103 at $\theta = \pi/3$; and 0.273 at $\pi/2$. That is, aliasing errors decrease the measured spectral index. Thus, if we use a nonlocal fitting

procedure to estimate p (as described below) and we wish to avoid using data that contributes local errors > 27% (or > 10.3%), we must discard half (or two-thirds) of the modes!

3.3 Estimating Spectral Indices of the Trapezoid

As discussed in Sec. 4, a least-squares (nonlocal) fitting procedure is used to estimate spectral indices. The essential caveats are: avoid using data near a transition between spectral ranges; and discard data above $k_{max}/2$ (or $k_{max}/3$). We discuss the choice of appropriate data fitting regions for the trapezoid, if we wish to obtain estimates of $p_2 = 2$ and $p_3 = 4$.

We wish to fit μ_3 peaks of the slow oscillation associated with sin $k(b-a)/2$ in the last region (No. 3). The last data mode will be

$$\gamma k_{max} \equiv \gamma\pi/h, \tag{3.10}$$

where, for example, to avoid aliasing errors $\gamma < 1/2$. If we start at $3\ k_2/2$, the condition for μ_3 peaks beyond the transition yields a range condition

$$\left(\frac{3}{2} + \mu_3\right)\left(2\pi/(b-a)\right) = \gamma\pi/h$$

or

$$(b - a) = h\left(3 + 2\mu_3\right)/\gamma. \tag{3.11}$$

The intermediate fitting region (No. 2) starts after k_1, the first null, and proceeds to k_1^*. Here k_1^* is chosen according to the error made as one approaches k_2, that is according to the departure of $[\sin (k(b - a)/2)/(k(b - a)/2)]^2$ from unity as given in

$$\left[\sin \tfrac{1}{2} k_1^*(b - a)/ \tfrac{1}{2} k_1^*(b-a)\right]^2 = 1 - \varepsilon_1{}^2 + O(\varepsilon_1{}^4),$$

or

$$\varepsilon_1 = (3)^{-1/2} k_1^*(b - a)/2, \tag{3.12}$$

We proceed as in the highest range, and require that we fit μ_2 peaks associated with $\sin k(b+a)/2$, or

$$\left(\tfrac{3}{2} + \mu_2\right)\left(2\pi/(b + a)\right) = (12)^{1/2} \varepsilon_1/(b - a), \tag{3.13}$$

or using (3.11)

$$(b + a) = h\left(3 + 2\mu_2\right)\left(3 + 2\mu_3\right) \pi/\gamma\varepsilon_1(12)^{1/2}. \tag{3.14}$$

Finally, we wish to have sufficient data in the first region before the first null at $2N/(\beta+\alpha)$. Thus

$$N = \mu_1(\beta + \alpha)/2, \tag{3.15}$$

where a minimal requirement is $\mu_1 > 4$. If we take $\mu_1 = 4$ and requirements in the other regions, as follows:

$$\mu_2 = \mu_3 = 3,\ \gamma = 1/2 \text{ and } \varepsilon_1{}^2 = 0.1, \tag{3.16}$$

then we obtain

$$(b - a)/h = 18, \ (b + a)/h = 464.6 \text{ and } N = 929,$$

where the last is obtained from (3.15). In Section 4.2 we will compare methods of fitting the data from the trapezoid $(b-a)/h = 16$ and $(b+a)/h = 464$ for $N = 512$, 1024, and 2048, which straddle the value $N = 929$.

4. FITTING DISCRETE DATA

4.1 Least Squares Fits

In this section we illustrate errors in a weighted least-squares fit of discrete data $|\hat{F}(k_\nu)|^2$ over specified ranges with

$$|\hat{F}_a|^2 = \overline{F}_a^2 \, k^{-\tilde{p}} = E_0 \, \nu^{-\tilde{p}}, \qquad \nu \, \varepsilon[-N+1, N]. \tag{4.1}$$

Thus, $\tilde{p}$ and E_0 are obtained from the pair of linear equations

$$\sum_\nu w_\nu \log_{10}|\hat{F}|^2 - \log_{10} E_0 \sum_\nu w_\nu + \tilde{p} \sum_\nu w_\nu z_\nu = 0 \tag{4.2}$$

$$\sum_\nu w_\nu z_\nu \log_{10}|\hat{F}|^2 - \log_{10} E_0 \sum_\nu w_\nu z_\nu + \tilde{p} \sum_\nu w_\nu z_\nu^2 = 0 \tag{4.3}$$

where $z_\nu = \log_{10}\nu$ and the weighting w_ν that yields good fits is

$$w_\nu = \frac{1}{2} \, |z_{\nu+1} - z_{\nu-1}| \quad \propto \quad \frac{1}{\nu} + O\left(\frac{1}{\nu^2}\right), \tag{4.4}$$

because it emphasizes the lower modes.

The fitting range for spectral region j is defined as

$$\nu \in [\nu_{jI}, \nu_{jF}]$$

where ν_{jI} and ν_{jF} are the initial and final mode values included in the fit for region j, and are chosen where $|\hat{F}(k_\nu)|^2$ has a local maximum, and such that they are not too close to transition points. This procedure was found to give a good estimate of $\tilde{p}$ for single figures. No consistent improvements were obtained when spectra for single figures were smoothed. However, when many figures were placed on a line (including overlapping figures), we found that the precise ν_{jI} and ν_{jF} were less critical. This follows because the point-to-point variation of $|\hat{F}|^2$ was large (i.e., poorly correlated). It is possible that an algorithm that fits $\log_{10}|\hat{F}|^2$ with a polynomial in z_ν would give a better estimate of a local spectral index.

Table 2 contains summary information on the top hat (a = b), circle (Eq. 2.8 with a = 0 and $\tau = 1/2$) and trapezoid. This table illustrates the errors made in obtaining $\tilde{p}$, when parameters are varied including the fitting interval $[\nu_{jI}\ \nu_{jF}]$ or n_{max}, the total number of data maxima in the interval. Measures of the quality of fit are given by $\delta_p = (\tilde{p} - p_j)/p_j \times 100$ and by

$$\bar{\sigma} = \frac{\{(\nu_{jF} - \nu_{jI})^{-1} \sum_\nu w_\nu(\log_{10}|\hat{F}|^2 - \log_{10} E_0\nu^{-\tilde{p}})^2\}^{1/2}}{[\sum_\nu w_\nu(z_\nu - \bar{z})^2]^{1/2}} \qquad (4.5)$$

where $\bar{z} = \sum_\nu w_\nu z_\nu / \sum_\nu w_\nu$. Note: In statistical fitting procedures $\bar{\sigma}$ is the square root of the variance of $\tilde{p}$.

Table 2 — Results of fitting simple figures

Type	Case	N	a/h	b/h	ν_I	ν_F	n_{max}	j	$\tilde{p}_j$	δ_p	$\bar{\sigma}$
Top Hat											
	1	2048	232	232	14	1038	111	2	2.06	3.0	0.04
	2	2048	232	232	14	526	56	2	2.10	5.0	0.07
	3	1024	232	232	8	528	99	2	2.04	2.0	0.06
	4	1024	232	232	8	268	50	2	2.09	4.5	0.11
	5	256	58	58	8	140	26	2	2.08	4.0	0.18
	6	256	58	58	8	74	13	2	2.23	11.5	0.34
Circle											
	7	1024	0	232	8	528	99	2	3.06	2.0	0.06
	8	1024	0	232	8	268	50	2	3.16	5.3	0.11
	9	256	0	58	8	140	26	2	3.09	3.0	0.18
	10	256	0	58	8	74	13	2	3.30	10.0	0.34
Trapezoid											
	11	2048	224	240	14	120	12	2	2.53	26.5	0.25
	12	2048	224	240	14	85	9	2	2.48	24.	0.35
	13	2048	224	240	388	900	3	3	4.01	0.25	0.45
	14	2048	224	240	388	644	2	3	4.82	21.	1.06
	15	1024	224	240	8	61	11	2	2.47	23.5	0.36
	16	1024	224	240	8	43	8	2	2.35	17.5	0.50
	17	1024	224	240	194	450	3	3	4.06	1.5	0.68
	18	1024	224	240	194	322	2	3	5.02	25.0	1.6
	19	512	112	120	8	43	8	2	2.35	17.5	0.52
	20	512	112	120	8	25	4	2	2.58	29.0	1.1
	21	512	112	120	194	322	2	3	4.38	9.5	1.6

4.2 Discussion of Fitted Results.

The results given in Table 2 are for the top hat (cases 1-6), the circle (cases 7-10) and the trapezoid (cases 11-21). To assure a good value of $\tilde{p}$ (to minimize δ_p), the figures were well resolved and occupied a small extent of the total interval (to yield well-defined oscillations). These requirements dictate a large total mesh size. The cases illustrated in the table show the effect of satisfying these criteria to a greater or lesser degree.

If we compare the errors in the least squares results for region 2 we find that for the top hat and circle (two-region functions) $\tilde{p}_2$ is much closer to p_2 than for the trapezoid (a three-region function), for a given mesh size. Thus, even with large-mesh sizes a least squares fit to the data produces substantial errors in the prediction of a spectral index if there are several distinct regions of k-space with different spectral indices.

Cases 1 and 2 show results for a mesh (2N = 4096) much larger than is being used presently in numerical simulations. A plot of $\log_{10}|\hat{F}|^2$ vs. $\log_{10}\nu$ for these cases is shown in Figure 2. The ordinate is normalized so that the area under the profile is unity. The lower scale on the abscissa is defined in such a way as to provide a measure of the size of the object relative to the mesh. The number given at the origin is the ratio of the mesh size to the size of the figure (here it is 8.8 = 2048/232). The first null (which is not, in general, a point of the plot) occurs at 1 on this scale, the second at 1/2, the third at 1/3, etc. In Table 2 we see errors, δ_p, in $\tilde{p}$ of 3% and 5%, respectively, and a consistent variation in $\bar{\sigma}$. Note that the fitting procedure always yields a $\tilde{p} > p$. This is due to our algorithm for choosing the fitting regions. We are not certain

whether the increase in error from case 1 to case 2 is related to the decrease in sample size (14-1038 to 14-526) or has to do with ν_{2F} in case 2 being farther from the aliasing region, since aliasing tends to spuriously reduce $\tilde{p}$. In any event, the errors are acceptably small. In cases 3 and 4 the same top hat is placed on a mesh half the size of that in cases 1 and 2. We obtain slightly better results, with errors of 2% and 4.5% respectively. The minor improvement is due to the particular choices of ν_{2I} and ν_{2F} determined by our algorithms. In fact, choosing ν_I in cases 1 and 2 to be 15 instead of 14 improves the fit enough that cases 1 and 2 then show smaller errors than cases 3 and 4, respectively.

With a smaller top hat in a smaller box (2N = 512, cases 5 and 6, Figure 3) the errors are larger, 4% for case 5 and 11.5% for case 6. The normalized standard deviation, $\bar{\sigma}$, has also increased. For the circular arc the results are consistent with the top hat results. For example, cases 7 and 8 give δ_p of 2% and 5%, respectively. The errors for cases 9 and 10 compare closely, also, with the analogous top hat cases 5 and 6.

For the trapezoid (see Figure 4), the errors in p_2 range from 17.5% to 29%. Generally, as the data set increases, δ_p and $\bar{\sigma}$ decrease if we do not approach too close to transitional points or aliasing regions. The smaller errors in region 3 are the result of aliasing errors competing with the errors introduced by the fitting procedure. The variation in δ_p for different meshes among comparable regions (e.g. 26.5%, 23.5% and 17.5%) is an indication of the magnitude of the variability obtained by such procedures when data with aliasing errors are included. These larger errors result because the configuration of "minimal" parameters (3.16) does

not yield a sufficient number of oscillations of data far from the transitional points. If we choose a more conservative set of parameters, e.g.

$$\mu_1 = 8, \qquad \mu_2 = \mu_3 = 4, \qquad \gamma = \frac{1}{3} \qquad \text{and} \qquad \varepsilon_1^{\;2} = 0.01$$

then we obtain

$$(b - a)/h = 33, \qquad (b + a)/h = 3290 \qquad \text{and} \qquad N = 13{,}170.$$

This large value of N cannot be used conveniently or routinely with present-day computers.

In addition to the trapezoid runs in Table 2 we have made runs with randomly placed multiple (three) identical trapezoids. In a mesh with $N = 2048$, analogous to the single trapezoid cases 11-14, we found only small differences in the resulting values of $\breve{p}_j$. This suggests that single figures can provide a good estimate of variability due to fitting procedures in a situation where multiple figures occur. However, a proper statistical theory for multiple figures is needed to generalize our limited findings.

5. CONCLUSIONS

We have demonstrated the essential elements which are required to determine accurate estimates of spectral indices. We have presented both analytical arguments and numerical experiments, which use least squares procedures for simple geometric representations of scan functions. For two-region figures, such as the top hat or circular arc, we find that an accurate estimate of the spectral index can be obtained with 256 or larger mode numbers, over a dynamical range of 30-50 db. However, for three-spectral region figures, even with a moderate separation of scales, an excess of 2048 modes is required to obtain good estimates of the spectral indices. Here, a typical dynamical range is 80 db. We have investigated various sources of errors including, for example, the number of modes in the data set, aliasing, and transitional nulls. It is possible that fitting functions, which are based on physical considerations, will reduce the data set required to obtain accurate estimates of spectral indices.

There is a practical lesson to be learned from this study. Spectral indices determined from data cannot safely be used beyond the range in k for which they have been measured. We have shown that even under well controlled conditions large errors in spectral indices can occur. To extrapolate these indices beyond the dynamical range for which they were obtained can produce power level predictions that are incorrect by orders of magnitude. From a systems perspective one could conceivably take a very conservative point of view, a worst case hypothesis, and assume that wherever the atmosphere structures, the spatial power spectrum of irregularities falls off like k^{-2}. However, this would be unduly constraining to instrument designers. The fact is that we do know a fair amount about the likely shapes of striations under HANE conditions. We

should, therefore, be able to construct analytical models of striations that sufficiently mimic reality so that we can investigate the sensitivity of spectral indices both to model parameters and to the direction of observation. Their validity could not go to larger k values than is warranted by the details of striation structures as predicted by our physical theories. These studies are being embarked upon now and will be reported on presently.

Acknowledgment

This work was supported by the Defense Nuclear Agency.

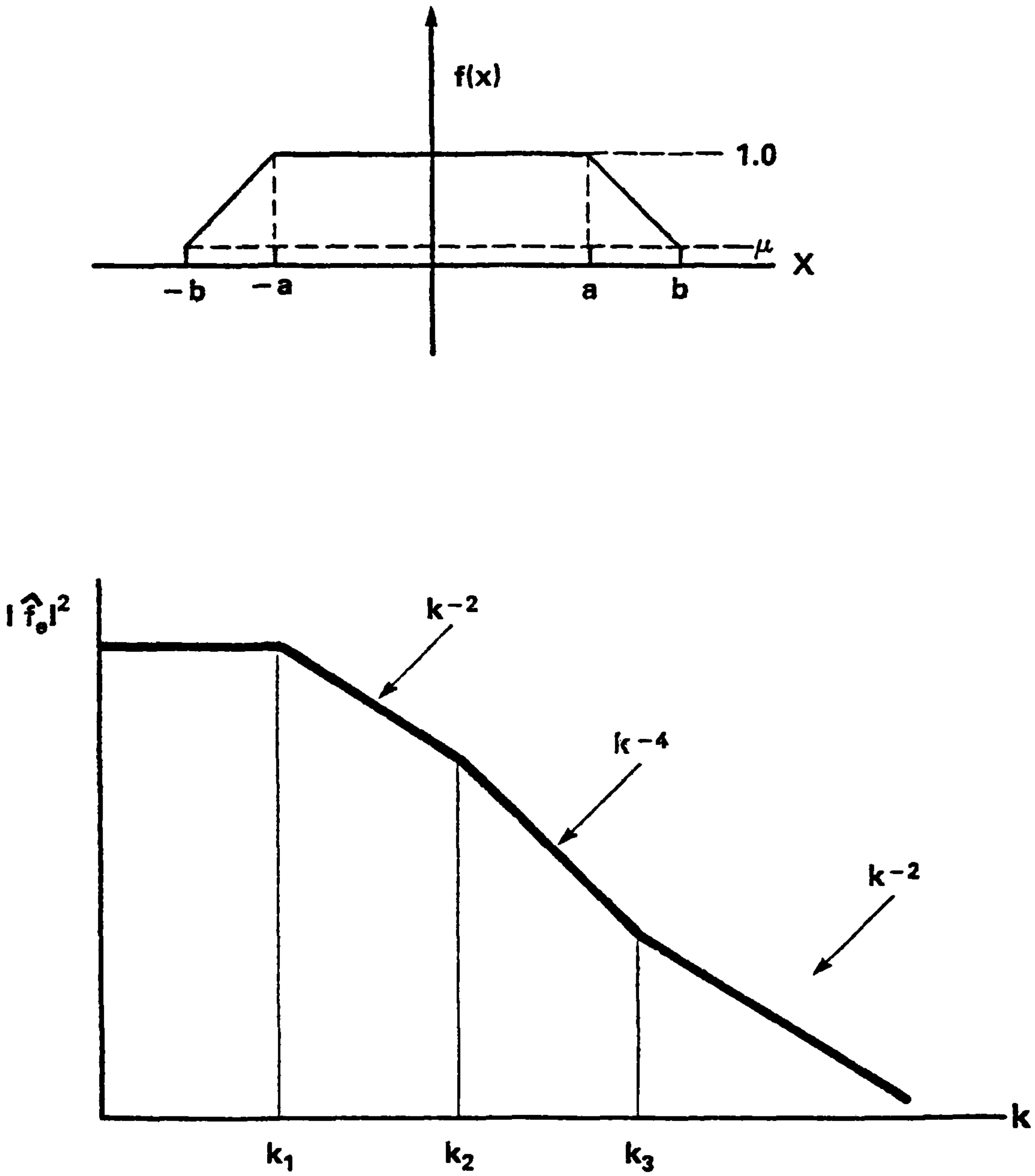

Fig. 1. An example of a function with four spectral regions.

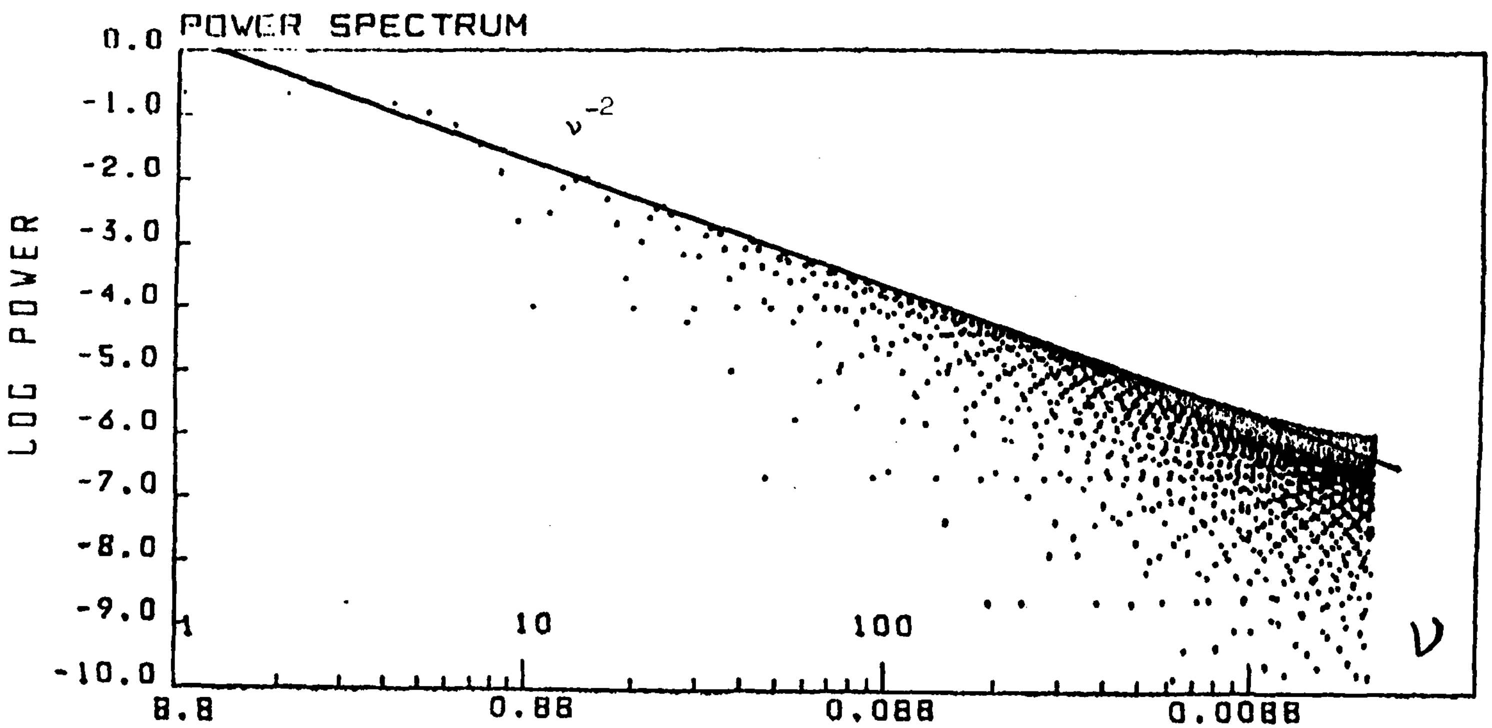

Fig. 2. Plot of $\log_{10}|\hat{F}|^2$ vs. $\log_{10}\nu$ for a top hat with N = 2048, a = b = 232. A straight line with slope -2 has been drawn through the second maximum.

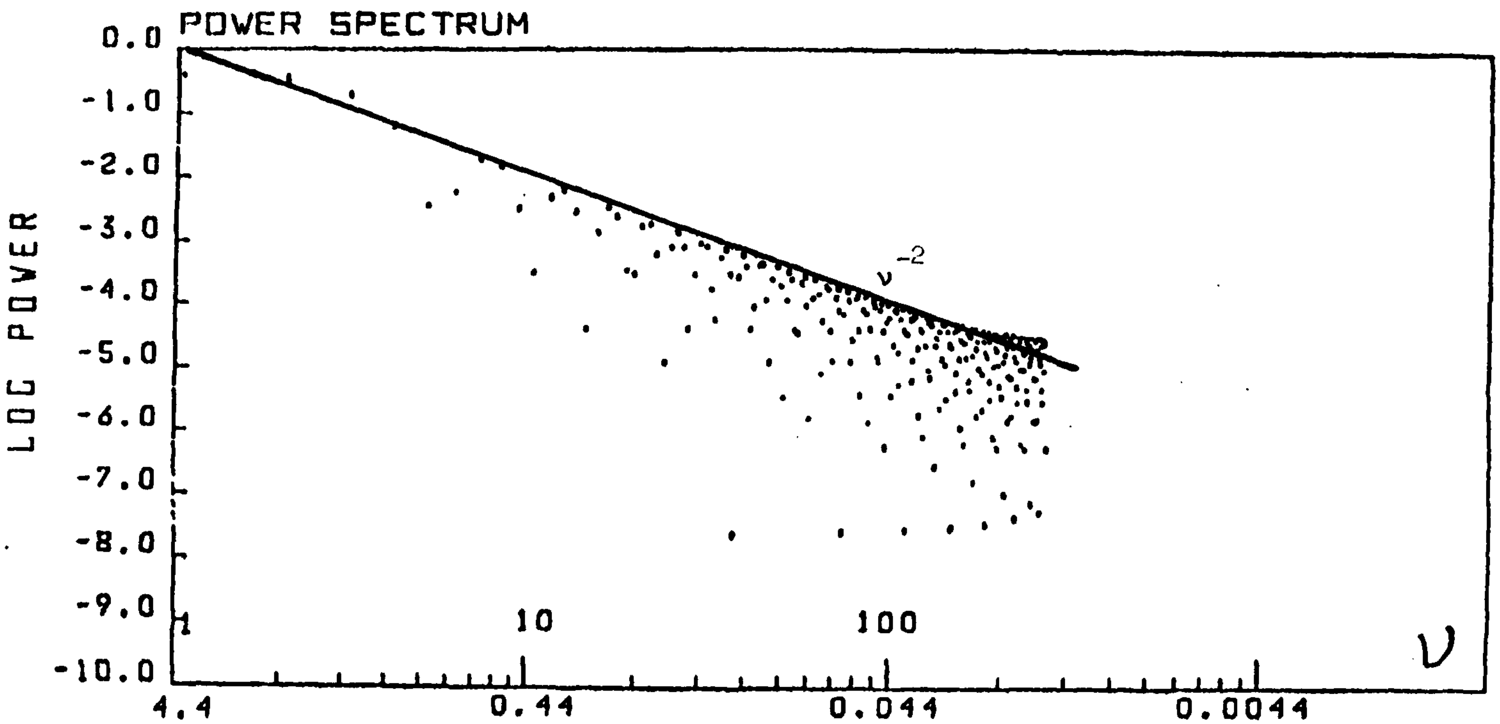

Fig. 3. Plot of $\log_{10}|\hat{F}|^2$ vs. $\log_{10}\nu$ for a top hat with N = 256, a = b = 58. A straight line with slope −2 has been drawn through the second maximum.

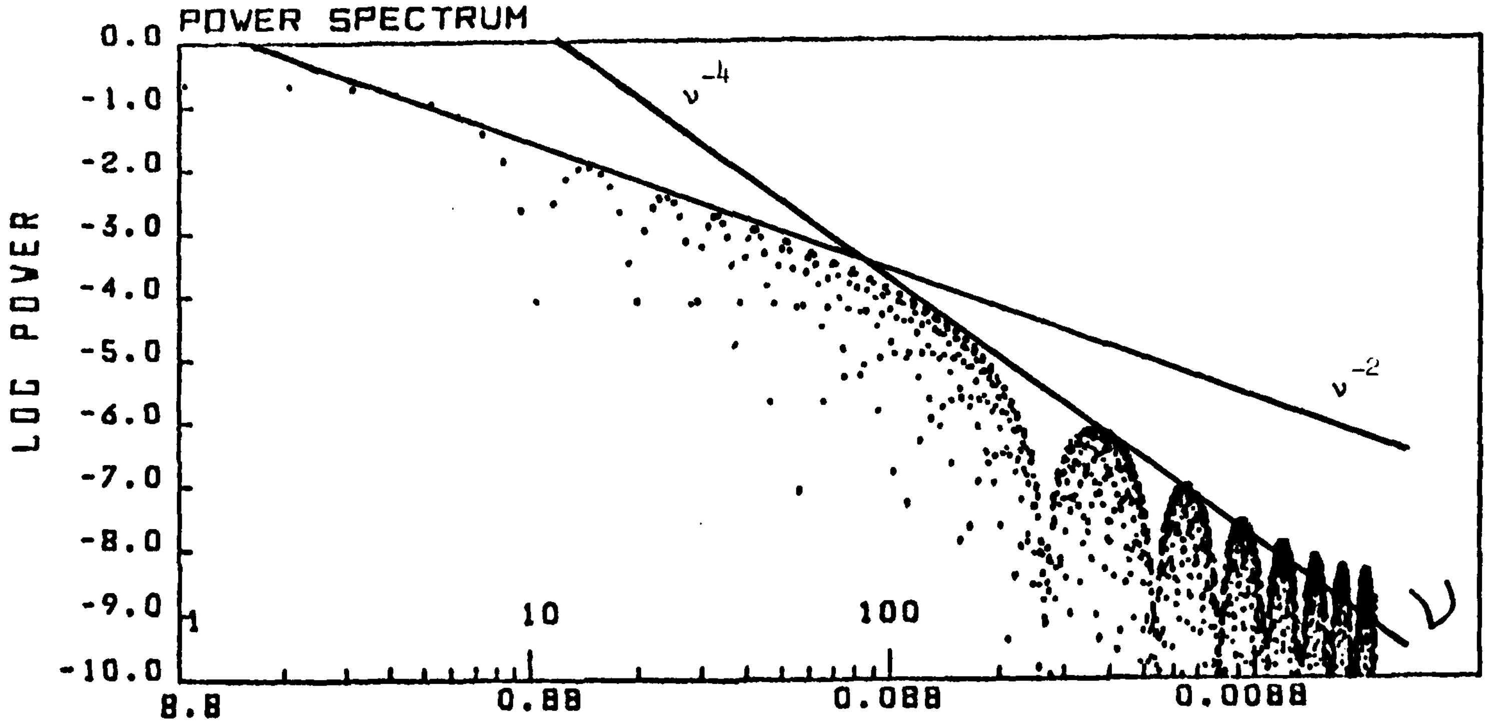

Fig. 4. Plot of $\log_{10}|\hat{F}|^2$ vs. $\log_{10}\nu$ for a trapezoid with N = 2048, a = 224, and b = 240. Straight lines with slopes of −2 and −4 have been drawn through the relevant second maxima.

APPENDIX A. TRANSFORM OF A SPECIAL FUNCTION

We consider the function

$$f(x) = 1 \qquad |x| < a,$$

$$f(x) = \left(1 - \Delta^{-2}(x - a)^2\right)^{\tau}, \qquad a < |x| < b,$$

$$f(x) = 0 \qquad |x| > b, \tag{A1}$$

where $\Delta = b - a$ and $\tau > 1$. Since it is symmetric the transform can be written as

$$\hat{f}(k) = I + I^* + 2k^{-1} \sin ka, \tag{A2}$$

where the last term is associated with the region $|x| < a$ and

$$I = \left\{\left(\tfrac{1}{2}\,\Delta\right)^{-\tau+1/2} \pi^{1/2}\Gamma(\tau+1)\; k^{-(\tau+1/2)}\; e^{-ika}\right\} \times$$

$$\left\{J_{\tau+1/2}(k\Delta) - i\, \underset{\sim}{H}_{\tau+1/2}(k\Delta)\right\}. \tag{A3}$$

The last is obtained from [5] Sec. 4.3, Eq. 12 and the use of

$$I_{\tau+1/2}(k\Delta) = i^{\tau+1/2}\; J_{\tau+1/2}(k\Delta),$$

and

$$\underset{\sim}{L}_{\tau+1/2}(ik\Delta) = i^{\tau+3/2}\; \underset{\sim}{H}_{\tau+1/2}(k\Delta),$$

where J_m and I_m are the usual Bessel functions and $\underset{\sim}{L}_m$ and $\underset{\sim}{H}_m$ are the Struve functions.

It can be shown that if $\Delta >> (b+a)/2$, $|\hat{f}(k)|^2$ has two well-separated spectral regions where the spectral index of the envelope is $p_1 = 2$ and $p_2 = 2(\tau+1)$, respectively. Thus, if $\tau = -1 + \varepsilon$ then $p_2 = 2\varepsilon$, nearly a flat spectrum.

REFERENCES

1. Wortman, W.R. and Kilb, R.W., Contact Geophysical and Plasma Dynamics Branch, Code 4780, NRL for Reference.

2. Brigham, E.O., The Fast Fourier Transform, Prentice Hall, Englewood Cliffs, N.J., 1974.

3. Abramowitz, M. and Stegun, I.A., Handbook of Mathematical Functions. See Sec. 12, and Eq. 12.1.31, National Bureau of Standards Applied Mathematical Series #55, 1964.

4. Koopmans, L.H., The Spectral Analysis of Time Series, Academic Press, N.Y., 1974. Aliasing is discussed in Chapter 3. It is also discussed in Reference 2, Chapter 6.

5. Erdelyi, A. (ed.), Tables of Integral Transforms, I., McGraw-Hill Book Co., Inc., N.Y., 1954.

DISTRIBUTION LIST

DEPARTMENT OF DEFENSE

ASSISTANT SECRETARY OF DEFENSE
COMM, CMD, CONT 7 INTELL
WASHINGTON, D.C. 20301

DIRECTOR
COMMAND CONTROL TECHNICAL CENTER
PENTAGON RM BE 685
WASHINGTON, D.C. 20301
01CY ATTN C-650
01CY ATTN C-312 R. MASON

DIRECTOR
DEFENSE ADVANCED RSCH PROJ AGENCY
ARCHITECT BUILDING
1400 WILSON BLVD.
ARLINGTON, VA. 22209
01CY ATTN NUCLEAR MONITORING RESEARCH
01CY ATTN STRATEGIC TECH OFFICE

DEFENSE COMMUNICATION ENGINEER CENTER
1860 WIEHLE AVENUE
RESTON, VA. 22090
01CY ATTN CODE R410
01CY ATTN CODE R812

DEFENSE TECHNICAL INFORMATION CENTER
CAMERON STATION
ALEXANDRIA, VA. 22314
02CY

DIRECTOR
DEFENSE NUCLEAR AGENCY
WASHINGTON, D.C. 20305
01CY ATTN STVL
04CY ATTN TITL
01CY ATTN DDST
03CY ATTN RAAE

COMMANDER
FIELD COMMAND
DEFENSE NUCLEAR AGENCY
KIRTLAND, AFB, NM 87115
01CY ATTN FCPR

DEFENSE NUCLEAR AGENCY
SAO/DNA
BUILDING 20676
KIRTLAND AFB, NM 87115
01CY D.C. THORNBURG

DIRECTOR
INTERSERVICE NUCLEAR WEAPONS SCHOOL
KIRTLAND AFB, NM 87115
01CY ATTN DOCUMENT CONTROL

JOINT CHIEFS OF STAFF
WASHINGTON, D.C. 20301
01CY ATTN J-3 WWMCCS EVALUATION OFFICE

DIRECTOR
JOINT STRAT TGT PLANNING STAFF
OFFUTT AFB
OMAHA, NB 68113
01CY ATTN JLTW-2
01CY ATTN JPST G. GOETZ

CHIEF
LIVERMORE DIVISION FLD COMMAND DNA
DEPARTMENT OF DEFENSE
LAWRENCE LIVERMORE LABORATORY
P.O. BOX 808
LIVERMORE, CA 94550
01CY ATTN FCPRL

COMMANDANT
NATO SCHOOL (SHAPE)
APO NEW YORK 09172
01CY ATTN U.S. DOCUMENTS OFFICER

UNDER SECY OF DEF FOR RSCH & ENGRG
DEPARTMENT OF DEFENSE
WASHINGTON, D.C. 20301
01CY ATTN STRATEGIC & SPACE SYSTEMS (OS)

WWMCCS SYSTEM ENGINEERING ORG
WASHINGTON, D.C. 20305
01CY ATTN R. CRAWFORD

COMMANDER/DIRECTOR
ATMOSPHERIC SCIENCES LABORATORY
U.S. ARMY ELECTRONICS COMMAND
WHITE SANDS MISSILE RANGE, NM 88002
01CY ATTN DELAS-EO F. NILES

DIRECTOR
BMD ADVANCED TECH CTR
HUNTSVILLE OFFICE
P.O. BOX 1500
HUNTSVILLE, AL 35807
  01CY ATTN ATC-T MELVIN T. CAPPS
  01CY ATTN ATC-O W. DAVIES
  01CY ATTN ATC-R DON RUSS

PROGRAM MANAGER
BMD PROGRAM OFFICE
5001 EISENHOWER AVENUE
ALEXANDRIA, VA 22333
  01CY ATTN DACS-BMT J. SHEA

CHIEF C-E- SERVICES DIVISION
U.S. ARMY COMMUNICATIONS CMD
PENTAGON RM 1B269
WASHINGTON, D.C. 20310
  01CY ATTN C- E-SERVICES DIVISION

COMMANDER
FRADCOM TECHNICAL SUPPORT ACTIVITY
DEPARTMENT OF THE ARMY
FORT MONMOUTH, N.J. 07703
  01CY ATTN DRSEL-NL-RD H. BENNET
  01CY ATTN DRSEL-PL-ENV H. BOMKE
  01CY ATTN J.E. QUIGLEY

COMMANDER
U.S. ARMY COMM-ELEC ENGRG INSTAL AGY
FT. HUACHUCA, AZ 85613
  01CY ATTN CCC-EMEO GEORGE LANE

COMMANDER
U.S. ARMY FOREIGN SCIENCE & TECH CTR
220 7TH STREET, NE
CHARLOTTESVILLE, VA 22901
  01CY ATTN DRXST-SD

COMMANDER
U.S. ARMY MATERIAL DEV & READINESS CMD
5001 EISENHOWER AVENUE
ALEXANDRIA, VA 22333
  01CY ATTN DRCLDC J.A. BENDER

COMMANDER
U.S. ARMY NUCLEAR AND CHEMICAL AGENCY
7500 BACKLICK ROAD
BLDG 2073
SPRINGFIELD, VA 22150
  01CY ATTN LIBRARY

DIRECTOR
U.S. ARMY BALLISTIC RESEARCH LABORATORY
ABERDEEN PROVING GROUND, MD 21005
  01CY ATTN TECH LIBRARY EDWARD BAICY

COMMANDER
U.S. ARMY SATCOM AGENCY
FT. MONMOUTH, NJ 07703
  01CY ATTN DOCUMENT CONTROL

COMMANDER
U.S. ARMY MISSILE INTELLIGENCE AGENCY
REDSTONE ARSENAL, AL 35809
  01CY ATTN JIM GAMBLE

DIRECTOR
U.S. ARMY TRADOC SYSTEMS ANALYSIS ACTIVITY
WHITE SANDS MISSILE RANGE, NM 88002
  01CY ATTN ATAA-SA
  01CY ATTN TCC/F. PAYAN JR.
  01CY ATTN ATTA-TAC LTC J. HESSE

COMMANDER
NAVAL ELECTRONIC SYSTEMS COMMAND
WASHINGTON, D.C. 20360
  01CY ATTN NAVALEX 034 T. HUGHES
  01CY ATTN PME 117
  01CY ATTN PME 117-T
  01CY ATTN CODE 5011

COMMANDING OFFICER
NAVAL INTELLIGENCE SUPPORT CTR
4301 SUITLAND ROAD, BLDG. 5
WASHINGTON, D.C. 20390
  01CY ATTN MR. DUBBIN STIC 12
  01CY ATTN NISC-50
  01CY ATTN CODE 5404 J. GALET

COMMANDER
NAVAL OCEAN SYSTEMS CENTER
SAN DIEGO, CA 92152
  01CY ATTN J. FERGUSON

NAVAL RESEARCH LABORATORY
WASHINGTON, D.C. 20375
01CY ATTN CODE 4700 S. L. Ossakow
26 CYS IF UNCLASS. 1 CY IF CLASS)
01CY ATTN CODE 4701 I Vitkovitsky
01CY ATTN CODE 4780 J. Huba (100
CYS IF UNCLASS, 1 CY IF CLASS)
01CY ATTN CODE 7500
01CY ATTN CODE 7550
01CY ATTN CODE 7580
01CY ATTN CODE 7551
01CY ATTN CODE 7555
01CY ATTN CODE 4730 E. MCLEAN
01CY ATTN CODE 4108
01CY ATTN CODE 4730 B. RIPIN
20CY ATTN CODE 2628

COMMANDER
NAVAL SEA SYSTEMS COMMAND
WASHINGTON, D.C. 20362
01CY ATTN CAPT R. PITKIN

COMMANDER
NAVAL SPACE SURVEILLANCE SYSTEM
DAHLGREN, VA 22448
01CY ATTN CAPT J.H. BURTON

OFFICER-IN-CHARGE
NAVAL SURFACE WEAPONS CENTER
WHITE OAK, SILVER SPRING, MD 20910
01CY ATTN CODE F31

DIRECTOR
STRATEGIC SYSTEMS PROJECT OFFICE
DEPARTMENT OF THE NAVY
WASHINGTON, D.C. 20376
01CY ATTN NSP-2141
01CY ATTN NSSP-2722 FRED WIMBERLY

COMMANDER
NAVAL SURFACE WEAPONS CENTER
DAHLGREN LABORATORY
DAHLGREN, VA 22448
01CY ATTN CODE DF-14 R. BUTLER

OFFICER OF NAVAL RESEARCH
ARLINGTON, VA 22217
01CY ATTN CODE 465
01CY ATTN CODE 461
01CY ATTN CODE 402
01CY ATTN CODE 420
01CY ATTN CODE 421

COMMANDER
AEROSPACE DEFENSE COMMAND/DC
DEPARTMENT OF THE AIR FORCE
ENT AFB, CO 80912
01CY ATTN DC MR. LONG

COMMANDER
AEROSPACE DEFENSE COMMAND/XPD
DEPARTMENT OF THE AIR FORCE
ENT AFB, CO 80912
01CY ATTN XPDQQ
01CY ATTN XP

AIR FORCE GEOPHYSICS LABORATORY
HANSCOM AFB, MA 01731
01CY ATTN OPR HAROLD GARDNER
01CY ATTN LKB KENNETH S.W. CHAMPION
01CY ATTN OPR ALVA T. STAIR
01CY ATTN PHD JURGEN BUCHAU
01CY ATTN PHD JOHN P. MULLEN

AF WEAPONS LABORATORY
KIRTLAND AFT, NM 87117
01CY ATTN SUL
01CY ATTN CA ARTHUR H. GUENTHER
01CY ATTN NTYCE 1LT. G. KRAJEI

AFTAC
PATRICK AFB, FL 32925
01CY ATTN TF/MAJ WILEY
01CY ATTN TN

AIR FORCE AVIONICS LABORATORY
WRIGHT-PATTERSON AFB, OH 45433
01CY ATTN AAD WADE HUNT
01CY ATTN AAD ALLEN JOHNSON

DEPUTY CHIEF OF STAFF
RESEARCH, DEVELOPMENT, & ACQ
DEPARTMENT OF THE AIR FORCE
WASHINGTON, D.C. 20330
01CY ATTN AFRDQ

HEADQUARTERS
ELECTRONIC SYSTEMS DIVISION
DEPARTMENT OF THE AIR FORCE
HANSCOM AFB, MA 01731
01CY ATTN J. DEAS

HEADQUARTERS
ELECTRONIC SYSTEMS DIVISION/YSEA
DEPARTMENT OF THE AIR FORCE
HANSCOM AFB, MA 01732
01CY ATTN YSEA

HEADQUARTERS
ELECTRONIC SYSTEMS DIVISION/DC
DEPARTMENT OF THE AIR FORCE
HANSCOM AFB, MA 01731
  01CY ATTN DCKC MAJ J.C. CLARK

COMMANDER
FOREIGN TECHNOLOGY DIVISION, AFSC
WRIGHT-PATTERSON AFB, OH 45433
  01CY ATTN NICD LIBRARY
  01CY ATTN ETDP B. BALLARD

COMMANDER
ROME AIR DEVELOPMENT CENTER, AFSC
GRIFFISS AFB, NY 13441
  01CY ATTN DOC LIBRARY/TSLD
  01CY ATTN OCSE V. COYNE

SAMSO/SZ
POST OFFICE BOX 92960
WORLDWAY POSTAL CENTER
LOS ANGELES, CA 90009
  (SPACE DEFENSE SYSTEMS)
  01CY ATTN SZJ

STRATEGIC AIR COMMAND/XPFS
OFFUTT AFB, NB 68113
  01CY ATTN ADWATE MAJ BRUCE BAUER
  01CY ATTN NRT
  01CY ATTN DOK CHIEF SCIENTIST

SAMSO/SK
P.O. BOX 92960
WORLDWAY POSTAL CENTER
LOS ANGELES, CA 90009
  01CY ATTN SKA (SPACE COMM SYSTEMS)
    M. CLAVIN

SAMSO/MN
NORTON AFB, CA 92409
(MINUTEMAN)
  01CY ATTN MNNL

COMMANDER
ROME AIR DEVELOPMENT CENTER, AFSC
HANSCOM AFB, MA 01731
  01CY ATTN EEP A. LORENTZEN

DEPARTMENT OF ENERGY
LIBRARY ROOM G-042
WASHINGTON, D.C. 20545
  01CY ATTN DOC CON FOR A. LABOWITZ

DEPARTMENT OF ENERGY
ALBUQUERQUE OPERATIONS OFFICE
P.O. BOX 5400
ALBUQUERQUE, NM 87115
  01CY ATTN DOC CON FOR D. SHERWOOD

EG&G, INC.
LOS ALAMOS DIVISION
P.O. BOX 809
LOS ALAMOS, NM 85544
  01CY ATTN DOC CON FOR J. BREEDLOVE

UNIVERSITY OF CALIFORNIA
LAWRENCE LIVERMORE LABORATORY
P.O. BOX 808
LIVERMORE, CA 94550
  01CY ATTN DOC CON FOR TECH INFO DEPT
  01CY ATTN DOC CON FOR L-389 R. OTT
  01CY ATTN DOC CON FOR L-31 R. HAGER
  01CY ATTN DOC CON FOR L-46 F. SEWARD

LOS ALAMOS NATIONAL LABORATORY
P.O. BOX 1663
LOS ALAMOS, NM 87545
  01CY ATTN DOC CON FOR J. WOLCOTT
  01CY ATTN DOC CON FOR R.F. TASCHEK
  01CY ATTN DOC CON FOR E. JONES
  01CY ATTN DOC CON FOR J. MALIK
  01CY ATTN DOC CON FOR R. JEFFRIES
  01CY ATTN DOC CON FOR J. ZINN
  01CY ATTN DOC CON FOR P. KEATON
  01CY ATTN DOC CON FOR D. WESTERVELT
  01CY ATTN D. SAPPENFIELD

SANDIA LABORATORIES
P.O. BOX 5800
ALBUQUERQUE, NM 87115
  01CY ATTN DOC CON FOR W. BROWN
  01CY ATTN DOC CON FOR A. THORNBROUGH
  01CY ATTN DOC CON FOR T. WRIGHT
  01CY ATTN DOC CON FOR D. DAHLGREN
  01CY ATTN DOC CON FOR 3141
  01CY ATTN DOC CON FOR SPACE PROJECT DIV

SANDIA LABORATORIES
LIVERMORE LABORATORY
P.O. BOX 969
LIVERMORE, CA 94550
  01CY ATTN DOC CON FOR B. MURPHEY
  01CY ATTN DOC CON FOR T. COOK

OFFICE OF MILITARY APPLICATION
DEPARTMENT OF ENERGY
WASHINGTON, D.C. 20545
  01CY ATTN DOC CON DR. YO SONG

OTHER GOVERNMENT

DEPARTMENT OF COMMERCE
NATIONAL BUREAU OF STANDARDS
WASHINGTON, D.C. 20234
 01CY (ALL CORRES: ATTN SEC OFFICER FOR)

INSTITUTE FOR TELECOM SCIENCES
NATIONAL TELECOMMUNICATIONS & INFO ADMIN
BOULDER, CO 80303
 01CY ATTN A. JEAN (UNCLASS ONLY)
 01CY ATTN W. UTLAUT
 01CY ATTN D. CROMBIE
 01CY ATTN L. BERRY

NATIONAL OCEANIC & ATMOSPHERIC ADMIN
ENVIRONMENTAL RESEARCH LABORATORIES
DEPARTMENT OF COMMERCE
BOULDER, CO 80302
 01CY ATTN R. GRUBB
 01CY ATTN AERONOMY LAB G. REID

DEPARTMENT OF DEFENSE CONTRACTORS

AEROSPACE CORPORATION
P.O. BOX 92957
LOS ANGELES, CA 90009
 01CY ATTN I. GARFUNKEL
 01CY ATTN T. SALMI
 01CY ATTN V. JOSEPHSON
 01CY ATTN S. BOWER
 01CY ATTN D. OLSEN

ANALYTICAL SYSTEMS ENGINEERING CORP
5 OLD CONCORD ROAD
BURLINGTON, MA 01803
 01CY ATTN RADIO SCIENCES

AUSTIN RESEARCH ASSOC., INC.
1901 RUTLAND DRIVE
AUSTIN, TX 78758
 01CY ATTN L. SLOAN
 01CY ATTN R. THOMPSON

BERKELEY RESEARCH ASSOCIATES, INC.
P.O. BOX 983
BERKELEY, CA 94701
 01CY ATTN J. WORKMAN
 01CY ATTN C. PRETTIE
 01CY ATTN S. BRECHT

BOEING COMPANY, THE
P.O. BOX 3707
SEATTLE, WA 98124
 01CY ATTN G. KEISTER
 01CY ATTN D. MURRAY
 01CY ATTN G. HALL
 01CY ATTN J. KENNEY

CHARLES STARK DRAPER LABORATORY, INC.
555 TECHNOLOGY SQUARE
CAMBRIDGE, MA 02139
 01CY ATTN D.B. COX
 01CY ATTN J.P. GILMORE

COMSAT LABORATORIES
LINTHICUM ROAD
CLARKSBURG, MD 20734
 01CY ATTN G. HYDE

CORNELL UNIVERSITY
DEPARTMENT OF ELECTRICAL ENGINEERING
ITHACA, NY 14850
 01CY ATTN D.T. FARLEY, JR.

ELECTROSPACE SYSTEMS, INC.
BOX 1359
RICHARDSON, TX 75080
 01CY ATTN H. LOGSTON
 01CY ATTN SECURITY (PAUL PHILLIPS)

EOS TECHNOLOGIES, INC.
606 Wilshire Blvd.
Santa Monica, Calif 90401
 01CY ATTN C.B. GABBARD

ESL, INC.
495 JAVA DRIVE
SUNNYVALE, CA 94086
 01CY ATTN J. ROBERTS
 01CY ATTN JAMES MARSHALL

GENERAL ELECTRIC COMPANY
SPACE DIVISION
VALLEY FORGE SPACE CENTER
GODDARD BLVD KING OF PRUSSIA
P.O. BOX 8555
PHILADELPHIA, PA 19101
 01CY ATTN M.H. BORTNER SPACE SCI LAB

GENERAL ELECTRIC COMPANY
P.O. BOX 1122
SYRACUSE, NY 13201
 01CY ATTN F. REIBERT

GENERAL ELECTRIC TECH SERVICES CO., INC.
HMES
COURT STREET
SYRACUSE, NY 13201
  01CY ATTN G. MILLMAN

GEOPHYSICAL INSTITUTE
UNIVERSITY OF ALASKA
FAIRBANKS, AK 99701
  (ALL CLASS ATTN: SECURITY OFFICER)
  01CY ATTN T.N. DAVIS (UNCLASS ONLY)
  01CY ATTN TECHNICAL LIBRARY
  01CY ATTN NEAL BROWN (UNCLASS ONLY)

GTE SYLVANIA, INC.
ELECTRONICS SYSTEMS GRP-EASTERN DIV
77 A STREET
NEEDHAM, MA 02194
  01CY ATTN DICK STEINHOF

HSS, INC.
2 ALFRED CIRCLE
BEDFORD, MA 01730
  01CY ATTN DONALD HANSEN

ILLINOIS, UNIVERSITY OF
107 COBLE HALL
150 DAVENPORT HOUSE
CHAMPAIGN, IL 61820
  (ALL CORRES ATTN DAN MCCLELLAND)
  01CY ATTN K. YEH

INSTITUTE FOR DEFENSE ANALYSES
1801 NO. BEAUREGARD STREET
ALEXANDRIA, VA 22311
  01CY ATTN J.M. AEIN
  01CY ATTN ERNEST BAUER
  01CY ATTN HANS WOLFARD
  01CY ATTN JOEL BENGSTON

INTL TEL & TELEGRAPH CORPORATION
500 WASHINGTON AVENUE
NUTLEY, NJ 07110
  01CY ATTN TECHNICAL LIBRARY

JAYCOR
11011 TORREYANA ROAD
P.O. BOX 85154
SAN DIEGO, CA 92138
  01CY ATTN J.L. SPERLING

JOHNS HOPKINS UNIVERSITY
APPLIED PHYSICS LABORATORY
JOHNS HOPKINS ROAD
LAUREL, MD 20810
  01CY ATTN DOCUMENT LIBRARIAN
  01CY ATTN THOMAS POTEMRA
  01CY ATTN JOHN DASSOULAS

KAMAN SCIENCES CORP
P.O. BOX 7463
COLORADO SPRINGS, CO 80933
  01CY ATTN T. MEAGHER

KAMAN TEMPO-CENTER FOR ADVANCED STUDIES
816 STATE STREET (P.O DRAWER QQ)
SANTA BARBARA, CA 93102
  01CY ATTN DASIAC
  01CY ATTN WARREN S. KNAPP
  01CY ATTN WILLIAM MCNAMARA
  01CY ATTN B. GAMBILL

LINKABIT CORP
10453 ROSELLE
SAN DIEGO, CA 92121
  01CY ATTN IRWIN JACOBS

LOCKHEED MISSILES & SPACE CO., INC
P.O. BOX 504
SUNNYVALE, CA 94088
  01CY ATTN DEPT 60-12
  01CY ATTN D.R. CHURCHILL

LOCKHEED MISSILES & SPACE CO., INC.
3251 HANOVER STREET
PALO ALTO, CA 94304
  01CY ATTN MARTIN WALT DEPT 52-12
  01CY ATTN W.L. IMHOF DEPT 52-12
  01CY ATTN RICHARD G. JOHNSON DEPT 52-12
  01CY ATTN J.B. CLADIS DEPT 52-12

MARTIN MARIETTA CORP
ORLANDO DIVISION
P.O. BOX 5837
ORLANDO, FL 32805
  01CY ATTN R. HEFFNER

M.I.T. LINCOLN LABORATORY
P.O. BOX 73
LEXINGTON, MA 02173
  01CY ATTN DAVID M. TOWLE
  01CY ATTN L. LOUGHLIN
  01CY ATTN D. CLARK

MCDONNEL DOUGLAS CORPORATION
5301 BOLSA AVENUE
HUNTINGTON BEACH, CA 92647
01CY ATTN N. HARRIS
01CY ATTN J. MOULE
01CY ATTN GEORGE MROZ
01CY ATTN W. OLSON
01CY ATTN R.W. HALPRIN
01CY ATTN TECHNICAL LIBRARY SERVICES

MISSION RESEARCH CORPORATION
735 STATE STREET
SANTA BARBARA, CA 93101
01CY ATTN P. FISCHER
01CY ATTN W.F. CREVIER
01CY ATTN STEVEN L. GUTSCHE
01CY ATTN R. BOGUSCH
01CY ATTN R. HENDRICK
01CY ATTN RALPH KILB
01CY ATTN DAVE SOWLE
01CY ATTN F. FAJEN
01CY ATTN M. SCHEIBE
01CY ATTN CONRAD L. LONGMIRE
01CY ATTN B. WHITE

MISSION RESEARCH CORP.
1720 RANDOLPH ROAD, S.E.
ALBUQUERQUE, NEW MEXICO 87106
01CY R. STELLINGWERF
01CY M. ALME
01CY L. WRIGHT

MITRE CORPORATION, THE
P.O. BOX 208
BEDFORD, MA 01730
01CY ATTN JOHN MORGANSTERN
01CY ATTN G. HARDING
01CY ATTN C.E. CALLAHAN

MITRE CORP
WESTGATE RESEARCH PARK
1820 DOLLY MADISON BLVD
MCLEAN, VA 22101
01CY ATTN W. HALL
01CY ATTN W. FOSTER

PACIFIC-SIERRA RESEARCH CORP
12340 SANTA MONICA BLVD.
LOS ANGELES, CA 90025
01CY ATTN E.C. FIELD, JR.

PENNSYLVANIA STATE UNIVERSITY
IONOSPHERE RESEARCH LAB
318 ELECTRICAL ENGINEERING EAST
UNIVERSITY PARK, PA 16802
(NO CLASS TO THIS ADDRESS)
01CY ATTN IONOSPHERIC RESEARCH LAB

PHOTOMETRICS, INC.
4 ARROW DRIVE
WOBURN, MA 01801
01CY ATTN IRVING L. KOFSKY

PHYSICAL DYNAMICS, INC.
P.O. BOX 3027
BELLEVUE, WA 98009
01CY ATTN E.J. FREMOUW

PHYSICAL DYNAMICS, INC.
P.O. BOX 10367
OAKLAND, CA 94610
- ATTN A. THOMSON

R & D ASSOCIATES
P.O. BOX 9695
MARINA DEL REY, CA 90291
01CY ATTN FORREST GILMORE
01CY ATTN WILLIAM B. WRIGHT, JR.
01CY ATTN ROBERT F. LELEVIER
01CY ATTN WILLIAM J. KARZAS
01CY ATTN H. ORY
01CY ATTN C. MACDONALD
01CY ATTN R. TURCO
01CY ATTN L. DeRAND
01CY ATTN W. TSAI

RAND CORPORATION, THE
1700 MAIN STREET
SANTA MONICA, CA 90406
01CY ATTN CULLEN CRAIN
01CY ATTN ED BEDROZIAN

RAYTHEON CO.
528 BOSTON POST ROAD
SUDBURY, MA 01776
01CY ATTN BARBARA ADAMS

RIVERSIDE RESEARCH INSTITUTE
330 WEST 42nd STREET
NEW YORK, NY 10036
01CY ATTN VINCE TRAPANI

SCIENCE APPLICATIONS, INC.
1150 PROSPECT PLAZA
LA JOLLA, CA 92037
01CY ATTN LEWIS M. LINSON
01CY ATTN DANIEL A. HAMLIN
01CY ATTN E. FRIEMAN
01CY ATTN E.A. STRAKER
01CY ATTN CURTIS A. SMITH
01CY ATTN JACK MCDOUGALL

SCIENCE APPLICATIONS, INC
1710 GOODRIDGE DR.
MCLEAN, VA 22102
ATTN: J. COCKAYNE

SRI INTERNATIONAL
333 RAVENSWOOD AVENUE
MENLO PARK, CA 94025
01CY ATTN DONALD NEILSON
01CY ATTN ALAN BURNS
01CY ATTN G. SMITH
01CY ATTN R. TSUNODA
01CY ATTN DAVID A. JOHNSON
01CY ATTN WALTER G. CHESNUT
01CY ATTN CHARLES L. RINO
01CY ATTN WALTER JAYE
01CY ATTN J. VICKREY
01CY ATTN RAY L. LEADABRAND
01CY ATTN G. CARPENTER
01CY ATTN G. PRICE
01CY ATTN R. LIVINGSTON
01CY ATTN V. GONZALES
01CY ATTN D. MCDANIEL

TECHNOLOGY INTERNATIONAL CORP
75 WIGGINS AVENUE
BEDFORD, MA 01730
01CY ATTN W.P. BOQUIST

TOYON RESEARCH CO.
P.O. Box 6890
SANTA BARBARA, CA 93111
01CY ATTN JOHN ISE, JR.
01CY ATTN JOEL GARBARINO

TRW DEFENSE & SPACE SYS GROUP
ONE SPACE PARK
REDONDO BEACH, CA 90278
01CY ATTN R. K. PLEBUCH
01CY ATTN S. ALTSCHULER
01CY ATTN D. DEE
01CY ATTN D/ STOCKWELL
SNTF/1575

VISIDYNE
SOUTH BEDFORD STREET
BURLINGTON, MASS 01803
01CY ATTN W. REIDY
01CY ATTN J. CARPENTER
01CY ATTN C. HUMPHREY

END

FILMED

5-84

DTIC